

All-electron local-density theory of covalently bonded material adsorbed on metallic substrate: $p(1 \times 1)$ Si monolayer on W(001)

Soon C. Hong, C. L. Fu, and A. J. Freeman

Department of Physics and Astronomy, Northwestern University, Evanston, Illinois 60208

(Received 20 April 1987; revised manuscript received 2 October 1987)

Results of self-consistent all-electron local-density-functional total-energy calculations of a Si monolayer on the W(001) surface employing the full-potential linearized augmented plane-wave method are presented. For an ordered $p(1 \times 1)$ overlayer of Si on the W(001) substrate we find a Si-W bond length of 2.59 Å, which is very close to that of bulk WSi_2 (2.62 Å). Surprisingly, compared to that of the clean W(001) the work function is not changed appreciably as a result of the covalent bonding. The strong covalent bonding between the Si and W atoms is found to suppress the localized surface states of the clean W(001) surface. Si-W interface bonding states are found at the symmetry points $\bar{\Gamma}$ and \bar{M} in the surface Brillouin zone with binding energies of -10.5 and -7.8 eV, respectively.

I. INTRODUCTION

There has been considerable interest in the study of the interaction between a covalently bonded material such as Si and a metallic substrate. Particular attention has focused on understanding the sharpness of the interface, the strength of chemical bonding, and possible compound formation near the metal-semiconductor interface.¹⁻⁶ While it is difficult to grow epitaxially macroscopic Si films on metallic substrates (due to the lack of sufficient surface mobility at low temperature and the rapid diffusion of Si atoms into the substrate at high temperature), the growth of Si overlayers on Al, Ni, Be, and Mo surfaces was reported over ten years ago.⁴⁻⁷ In general, more than five or six atomic layers of Si deposited on the metallic substrate resulted in amorphous films. However, the first few layers deposited at room temperature are found to be ordered: to cite a few examples, an 8×2 structure on Al(110); a 3×3 structure on Al(111);⁴ a $c(2 \times 2)$ structure on Ni(001); a $c(8 \times 2)$ structure on Ni(110); $\sqrt{3} \times \sqrt{3}$ (-30°), 2×2 , and 2×12 structures on Ni(111) with the increasing Si coverage;⁵ $\sqrt{3} \times \sqrt{3}$ (-30°) structure on Be(0001).⁶ More to the subject of this paper, it was reported that a monolayer of Si deposited on a clean Mo(001) surface is adsorbed in the fourfold pyramidal hollow sites formed by four adjacent Mo atoms on the Mo(001) substrate [as determined by low-energy electron diffraction (LEED)],⁷ i.e., to form a $p(1 \times 1)$ structure. More recently, it was shown by photoemission and Auger spectroscopy⁸ that Si interacts strongly with W and forms a WSi_2 structure at the Si-W(110) interface for up to ten monolayers of evaporated Si. Thus, it is of interest to study theoretically the electronic properties of a Si overlayer on W(001) at its initial stage of growth.

In this paper, we present an all-electron local-density-functional (LDF) (Refs. 9 and 10) total-energy study of the structural and electronic properties of a $p(1 \times 1)$ Si monolayer on the W(001) substrate [Si/W(001)] using the full-potential linearized augmented plane-wave (FLAPW) approach.¹¹ We employed a $p(1 \times 1)$ monolayer of Si on

a three-layer W(001) slab (to study the structural properties) and on a nine-layer W(001) substrate (to investigate the electronic properties). The results of these calculations were analyzed to yield information on bond formation and bonding character between the adsorbed $p(1 \times 1)$ Si monolayer and W(001) surface.

II. METHODOLOGY AND COMPUTATIONAL MODELS

To explore the structural properties of Si/W(001), we model the system by a single slab consisting of a three-layer W(001) with the $p(1 \times 1)$ Si monolayer adsorbed on each surface. The number of W layers is extended to nine to study possible thin-film size effects on the electronic properties. The experimental lattice constant of bulk bcc tungsten ($a = 3.16$ Å) is used and no surface relaxation of W(001) is included; the Si atoms are located above the fourfold hollow sites in the surface W layer, and the Si-W bond length is determined from total-energy calculations. [Note that this geometry is similar to that of a $p(1 \times 1)$ Si monolayer on the Mo(001) surface (isoelectronic to W) with a Si-Mo bond length of 2.51 ± 0.05 Å (as determined from LEED).⁷]

The local-density-functional one-particle equations are solved self-consistently using the FLAPW thin-film method. In this method no shape approximations are made to the electronic charge density and potential, and all matrix elements corresponding to this general potential are rigorously taken into account in all parts of space. The wave functions are expanded variationally in a basis set containing about 2×40 basis functions per atom. Self-consistency is assumed when the root-mean-square difference between input and output charge densities is less than 0.5×10^{-3} electrons/(a.u.)³. The core states are treated fully relativistically, and the valence states are calculated semirelativistically, i.e., spin-orbit coupling is neglected.¹² The $5p$ electrons of W are treated as band electrons in the present calculations (i.e., $5p$ polarization is allowed). We take the explicit form of Hedin and

Lundqvist¹³ as the exchange-correlation potential. The lattice harmonics with angular momentum up to $l = 8$ are included in expanding the charge density and potential and in constructing the wave functions inside the muffin-tin (MT) sphere.

III. RESULTS AND DISCUSSION

A. Total-energy studies: Structural properties

To study the bonding character of Si—W, we first have to know the bond length of a $p(1 \times 1)$ Si overlayer on the W(001) surface. Figure 1 shows the calculated total energy (E_T) as a function of the Si—W bond length. The dots represent the calculated values and the equilibrium height is then determined by least-squares fitting of a Lennard-Jones-type potential to the calculated result (solid line). The anharmonic effects can be considered due to the strong interaction between Si and W. As discussed later, this behavior is directly related to the bonding character between Si and W. From our calculation, we obtain a Si—W equilibrium bond length of 2.59 Å which is very close to that found experimentally (2.62 Å) (Ref. 14) for bulk WSi_2 (a theoretical calculation using the pseudopotential method found two inequivalent W—Si bond lengths of 2.61 and 2.63 Å).^{15,16} This result is consistent with the recent experimental finding that the adsorbed Si atoms interact strongly with the W(110) substrate and form the bulk WSi_2 structure at the interface.⁸

It is interesting to note that the refractory metals (Cr, Mo, W, and V) form Si-rich silicides at the metal-Si interfaces while the near noble metals (Pd, Pt, Cu, Ag, and Au) form metal-rich silicides.¹⁷ To examine the possibility of the diffusion of Si into the W surface layer, we also calculate the total energy of the slab with an ordered $p(1 \times 1)$ subsurface layer while keeping the Si—W bond

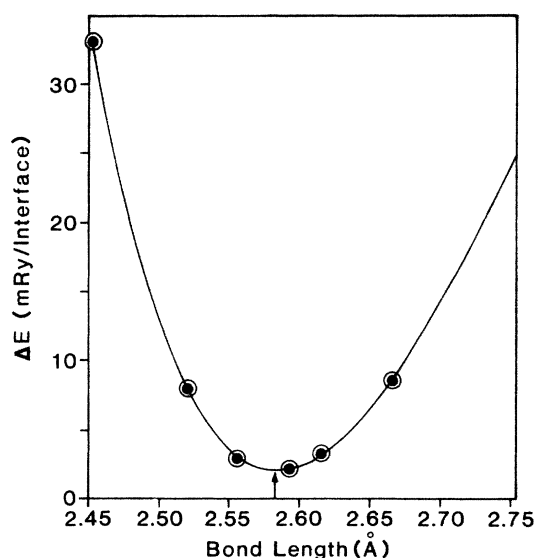


FIG. 1. Total energy of a $p(1 \times 1)$ Si overlayer on the three-layer W(001) slab as a function of the Si—W bond length. The circles are calculated data points fitted by a Lennard-Jones-type potential (solid line). The arrow denotes the minimum at 2.59 Å.

length at its equilibrium value (i.e., by interchanging the layer stacking sequence of the W surface layer and the Si overlayer for the overlayer case). We found that having the Si as a subsurface has a higher total energy ($\Delta E = 186$ meV) with respect to that of the Si as an overlayer at equilibrium. Hence, our result indicates that a Si overlayer formation at the interface tends to lower the interface energy, and, therefore, favors epitaxial growth.

B. Charge density and work function

In this section we discuss the charge density and work function because they have direct physical significance when obtained with LDF theory. Figure 2 shows the electronic valence charge-density contour map on the (110) plane for the upper half of the nine-layer W(001) slab with a Si monolayer adsorbed on each surface. As shown, the charge-density contours of the subsurface W ($S - 1$) layer is nearly the same as that of the inner layers. The effect of the adsorbed Si layers is shown to be mostly confined at the interface due to the short-ranged metallic screening.

Knowing the charge redistribution as a result of the adsorbed Si layers will give us some insight into the Si—W bonding character. To see the charge redistribution we subtract the superposed densities of an unsupported Si

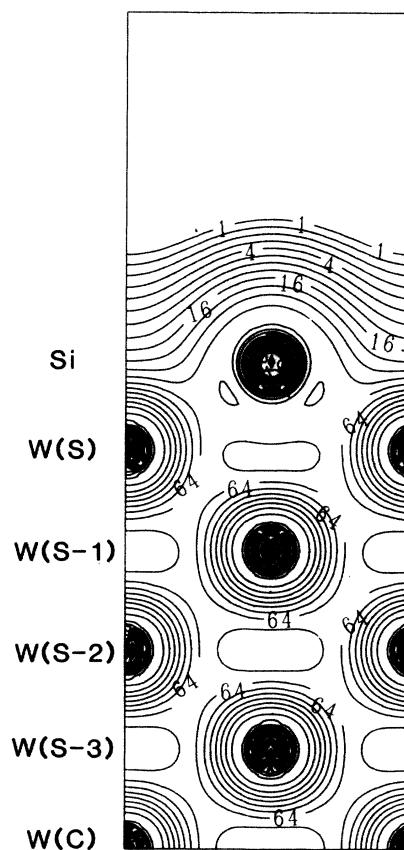


FIG. 2. Valence-electron charge density of a $p(1 \times 1)$ Si overlayer on the nine-layer W(001) slab in the (110) plane perpendicular to the surface in units of 10^{-3} electrons/(a.u.)³.

monolayer [with the same two-dimensional lattice constant as that of Si/W(001)] and the clean W(001) surface from the self-consistent valence charge density of Si/W(001). The difference of these charge densities is shown in Fig. 3, where the solid (dotted) line represents positive (negative) electronic charge-density differences. One noticeable feature from this charge-density difference plot is that the increase of charge is mainly centered in the middle of the Si—W bond, indicating strong covalent bonding. The small amount of charge transfer between Si and W and the covalent nature of Si—W bonding do not cause much modification of the W surface potential so that the resulting work function (4.60 eV) is not strongly affected by the presence of a Si overlayer from that calculated for the clean W(001) surface (4.62 eV).¹⁸ An experiment for a Si overlayer on W(110) (Ref. 8) also showed that work function decreases by a small amount (≤ 0.1 eV) at the initial stage of Si evaporation.

C. Bonding states and interface resonance states

Consider first the layer-projected density of states (LDOS) as a way to examine the effects of the presence of a Si overlayer on the electronic structure of the clean W(001) surface. Figure 4 shows the LDOS of the Si and W layers at the interface, and for comparison the center W(001) layer, and an unsupported Si monolayer with the

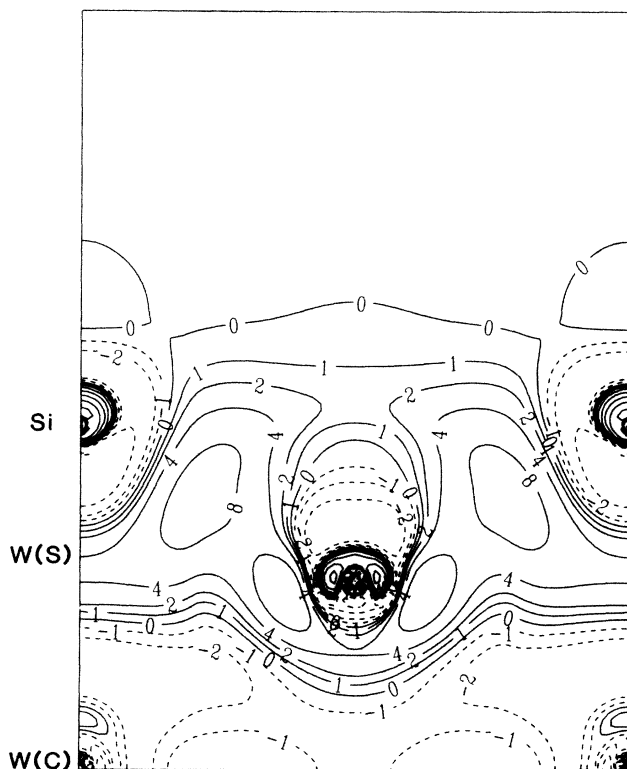


FIG. 3. Difference charge density of the $p(1 \times 1)$ Si/W(001) and the superposed W(001) plus a supported Si monolayer in units of 10^{-3} electrons/(a.u.)³. The solid (dotted) line indicates positive (negative) electronic charge density.

same lattice constant as that of Si/W(001).

Neither the unsupported Si monolayer nor the Si overlayer has a gap at the Fermi energy which is present in the bulk Si due to tetrahedral sp^3 hybridization. According to Pauling's criterion of bond strength,¹⁹ the sp^3 hybridization is no longer favored in the two-dimensional (2D) square lattice structure. Furthermore, the Si—Si bond length (3.16 Å) in this case is too large to permit interaction between s and p states of the Si atoms (the nearest-neighbor distances in bulk Si and WSi_2 are 2.35 and 2.63 Å, respectively). Thus, two of the four valence electrons of a Si atom in the unsupported Si monolayer occupy $3s$ states and the others partially fill the $3p$ band, keeping the gap between the $3s$ and $3p$ bands as shown in Fig. 4(d), unlike the case of bulk Si and WSi_2 .^{15,16} The valence electrons in the unsupported Si monolayer spill out into the vacuum to reduce their kinetic energy. Furthermore, one of the two $3p$ states is p_z -like so as to project farther into vacuum; the other $3p$ electron favors occupying a p_x or p_y state.

It is well known that there are certain distinct features which originate from the coupling between Si p states and metal d orbitals in a bulk metal silicide.^{15,16,20–24} In particular, the calculated atom-projected density of states of bulk WSi_2 (Refs. 15 and 16) indicates that the Si p states hybridize with the W d bands at binding energies (E_B) of 2.7 and 6.8 eV at the symmetry point of Γ in the $3d$ Brillouin zone. However, in our calculations for a $p(1 \times 1)$ Si monolayer on W(001), the Si p –W d hybridization feature is not obvious, as shown in Fig. 4(b). In the bulk metal silicide, the $3p$ electrons of the Si atoms are directed toward W atoms so as to form a Si $p\sigma$ bond with the d electrons [here we take (110) as the xy plane]. However, p electrons of the overlayer Si would spill out into the vacuum like the unsupported Si monolayer so that the directed Si p –W d bond should be weaker; Si p –W d hybridization should be restored with an increasing number of Si overlayers. Instead of the decrease of Si p –W d bond strength, the coupling of Si s states with W s and d bands becomes obvious and strong, as shown in Figs. 4(a) and 4(b). For the monolayer Si coverage the Si s –W d and/or –W s hybridization is responsible for the Si—W bonding.

The feature with a binding energy ($E_B = 7.8$ eV) in the LDOS of the Si overlayer [Fig. 4(a)] and W surface [Fig. 4(b)] is identified as due to Si—W bonding states, as seen by comparison to Figs. 4(c) and 4(d), and originates from the hybridization of a Si s state and W d band. The feature with a higher binding energy ($E_B = 10.5$ eV) is an s -like state, coming from the hybridization of W and Si s bands; the one with a lower binding energy ($E_B = 7.8$ eV) originates from the coupling of Si s states with d bands. Electrons in the bonding states at the lower binding energy are mostly responsible for the covalent bonding between the W and Si atoms. In contrast, the surface resonance states of W(001) along the $\Gamma\bar{X}$ direction (mostly d_{z^2} -type symmetry) are not strongly influenced by the Si overlayer. These states contribute to the peak just below E_F in the LDOS of the interface W layer.

Figure 5 displays the energy-band dispersions of

Si/W(001) along the high-symmetry lines of the irreducible 2D Brillouin zone. The top (bottom) panel represents odd (even) parity states with respect to the given symmetry plane normal to the surface. Dashed (dotted) lines indicate even (odd) parity states with respect to the mirror reflection in the central plane of the film. The interface states, which are defined by a localization of more than 35% in the interface W layer, are represented by solid lines. The bonding state at \bar{M} (the

localization of its wave function is more than 75% at the interface), corresponding to the feature with $E_B = 7.8$ eV in the LDOS of the Si overlayer and the surface W layer, shows no dispersion. On the other hand, the states around $\bar{\Gamma}$ ($E_B = 10.5$ eV) show upward parabolic dispersion with increasing k (i.e., s -like state).

The charge-density contour maps of these bonding states at \bar{M} and $\bar{\Gamma}$ are displayed in Figs. 6(a) and 6(b), respectively. These figures also display clearly that the

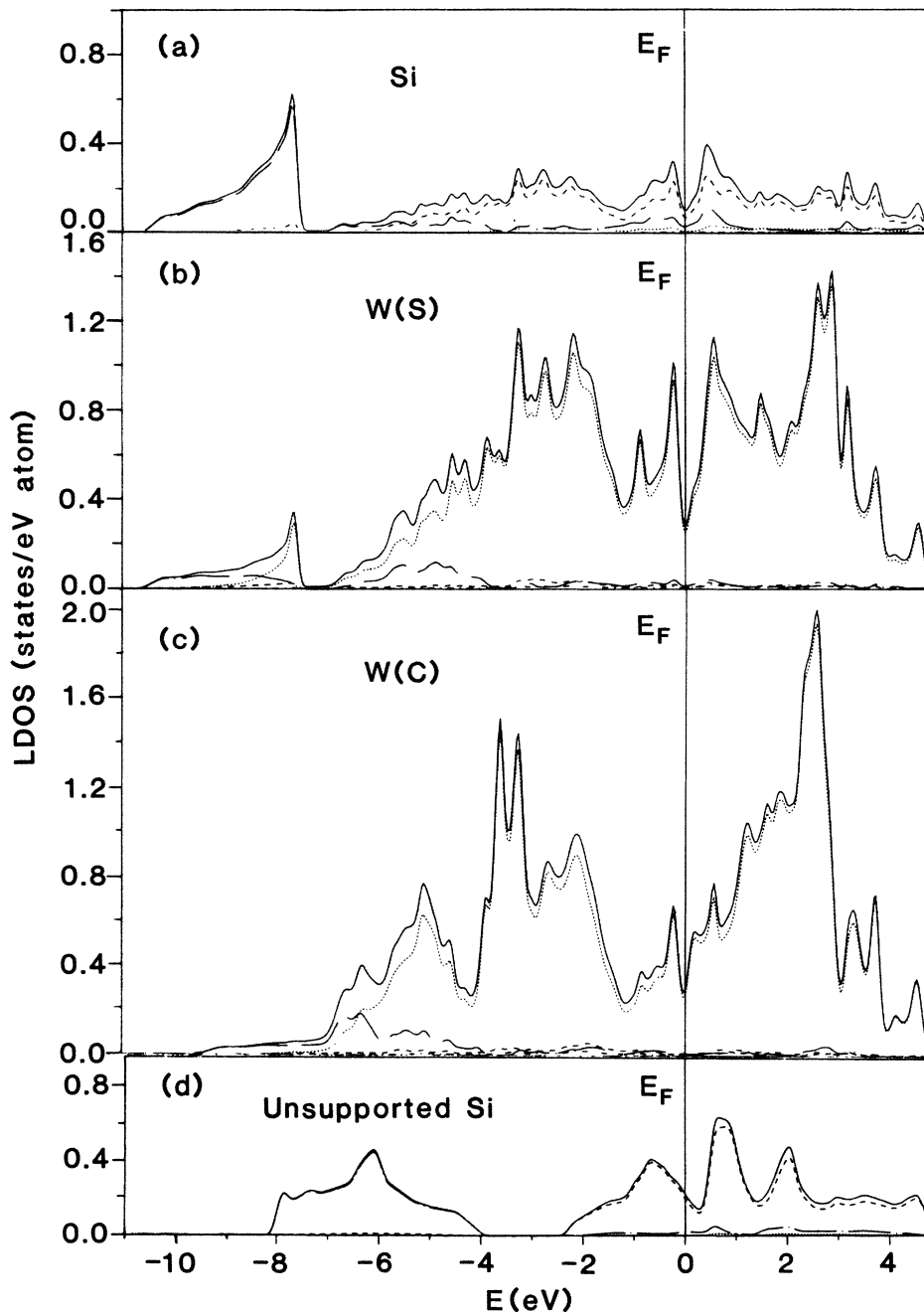


FIG. 4. Layer-projected partial density of states in units of states/eV atom for (a) Si and (b) W layers at the interface, (c) the center W layer, and (d) an unsupported Si monolayer with the same 2D lattice constant as that of Si/W(001). Solid lines represent the total LDOS; dashed-dotted lines the S component; dashed lines the p component; and dotted lines the d component of the LDOS, respectively.

states are very localized at the Si/W(001) interface and decay very rapidly into the W and that the states with the lower binding energy are most responsible for the bonding character. As mentioned already, the notable localized surface states (along the [110] direction) of W(001) (which are responsible for the surface reconstruction)²⁵ are completely eliminated upon Si adsorption.

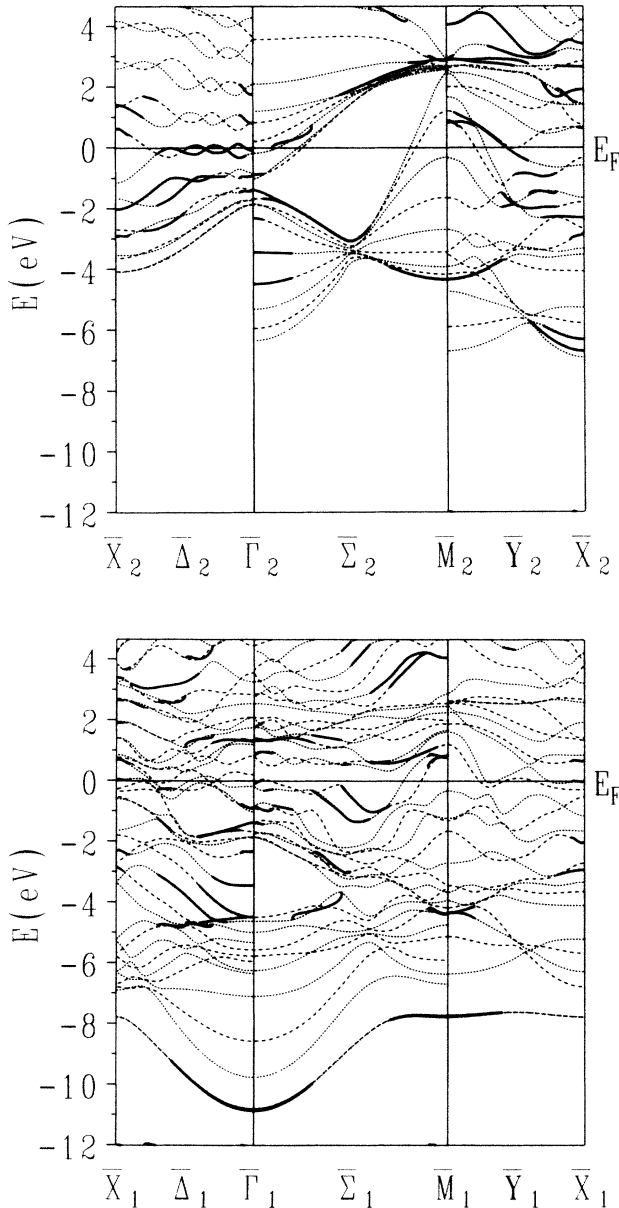


FIG. 5. Energy band for a $p(1 \times 1)$ Si overlayer on the nine-layer W(001) slab along high-symmetry lines in the 2D Brillouin zone. Top and lower panels show odd and even symmetries with respect to the given symmetry plane normal to the surface. Dashed and dotted lines represent even and odd parities with respect to z reflection. Solid lines indicate the interface states whose wave functions have more than 35% weight in the interface W layer.

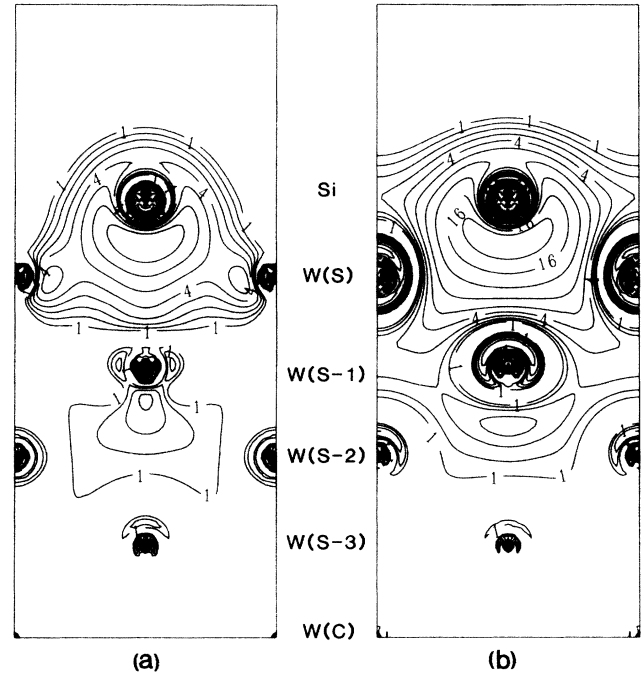


FIG. 6. Electronic charge density for the bonding states around the symmetry points (a) \bar{M} [in units of 10^{-3} electrons/(a.u.)³] and (b) $\bar{\Gamma}$ [in units of 10^{-4} electrons/(a.u.)³].

IV. SUMMARY AND CONCLUSION

We have studied the structural and electronic properties of a $p(1 \times 1)$ Si monolayer on a W(001) surface using highly precise FLAPW total-energy calculations within local-density-functional theory. Si/W(001) was represented by the single-slab geometry consisting of a W(001) film with a Si monolayer on either side.

The Si monolayer in an ordered overlayer on the W(001) substrate was found to form a bond length (2.59 Å) which is very close to that of bulk WSi_2 (2.62 Å). The localized surface states of clean W(001) are found to be suppressed by the presence of the strong covalent bonding between W surface atoms and Si. The most prominent bonding states found are (1) near the \bar{M} point of the 2D surface Brillouin zone with $E_B = 7.8$ eV (W d —Si s bonding), and (2) an s -like band near the $\bar{\Gamma}$ point with $E_B = 10.5$ eV (W s —Si s bonding).

Furthermore, the surface resonance states, which have d_{z^2} orbital character, are found to disperse along the symmetry line $\bar{\Gamma}\bar{X}$ near E_F . The work function is not changed appreciably by the presence of a Si overlayer compared to that of the clean W(001) surface.

ACKNOWLEDGMENTS

This work was supported by the Office of Naval Research (ONR) (Grant No. N00014-81K-0438) and by an ONR grant of computer time on the NRL Cray. We are grateful to John Weaver for suggesting this study and for encouragement.

- ¹J. J. Lander, *Prog. Solid State Chem.* **2**, 26 (1965), and references therein.
- ²B. Egert and G. Panzner, *Phys. Rev. B* **29**, 2091 (1984).
- ³B. Egert, H. J. Grabke, Y. Sakisaka, and T. N. Rhodin, *Surf. Sci.* **141**, 397 (1984).
- ⁴F. Jona, *J. Appl. Phys.* **42**, 2557 (1971).
- ⁵F. Jona, *J. Appl. Phys.* **44**, 351 (1973).
- ⁶F. Jona, *J. Appl. Phys.* **44**, 4240 (1973).
- ⁷A. Ignatiev, F. Jona, D. W. Jepsen, and P. W. Marcus, *Phys. Rev. B* **11**, 4780 (1975).
- ⁸S.-L. Weng, *Phys. Rev. B* **29**, 2363 (1984).
- ⁹P. Hohenberg and W. Kohn, *Phys. Rev.* **136**, B864 (1964).
- ¹⁰W. Kohn and L. J. Sham, *Phys. Rev.* **140**, A1133 (1965).
- ¹¹E. Wimmer, H. Krakauer, M. Weinert, and A. J. Freeman, *Phys. Rev. B* **24**, 864 (1981), and references therein.
- ¹²D. D. Koelling and B. N. Harmon, *J. Phys. C* **10**, 3107 (1977).
- ¹³L. Hedin and B. I. Lundqvist, *J. Phys. C* **4**, 2064 (1971).
- ¹⁴W. Zachariasen, *Z. Phys. Chem. (Leipzig)* **128**, 39 (1927).
- ¹⁵B. K. Bhattacharyya, D. M. Bylander, and L. Kleiman, *Phys. Rev. B* **31**, 2049 (1985).
- ¹⁶B. K. Bhattacharyya, D. M. Bylander, and L. Kleiman, *Phys. Rev. B* **32**, 7973 (1985).
- ¹⁷C. Calandra, O. Bisi, and G. Ottaviani, *Surf. Sci. Rep.* **4**, 271 (1985), and references therein.
- ¹⁸S. Ohnishi, A. J. Freeman, and E. Wimmer, *Phys. Rev. B* **29**, 5267 (1984).
- ¹⁹M. Tinkham, *Group Theory and Quantum Mechanics* (McGraw-Hill, New York, 1964), p. 87.
- ²⁰A. Franciosi and J. H. Weaver, *Surf. Sci.* **132**, 324 (1983).
- ²¹A. Franciosi and J. H. Weaver, *Phys. Rev. B* **27**, 3554 (1983).
- ²²A. Franciosi, J. H. Weaver, D. G. O'Neill, F. A. Schmidt, O. Bisi, and C. Calandra, *Phys. Rev. B* **28**, 7000 (1983).
- ²³J. H. Weaver, V. L. Moruzzi, and F. A. Schmidt, *Phys. Rev. B* **23**, 2916 (1981).
- ²⁴O. Bisi, L. W. Chiao, and K. N. Tu, *Phys. Rev. B* **30**, 4664 (1984).
- ²⁵C. L. Fu, A. J. Freeman, E. Wimmer, M. Weinert, *Phys. Rev. Lett.* **54**, 2261 (1985).